J|A|C|S
ARTICLES
Published on Web 07/27/2002

Contribution of Aromatic Interactions to α-Helix Stability

Sara M. Butterfield, Paresma R. Patel, and Marcey L. Waters*

Contribution from the Department of Chemistry, UNC Chapel Hill, Venable and Kenan Laboratories, CB 3290, Chapel Hill, North Carolina 27599

Received April 24, 2002

Abstract: The influence of natural and unnatural *i*, *i* + 4 aromatic side chain−side chain interactions on α-helix stability was determined in Ala-Lys host peptides by circular dichroism (CD). All interactions investigated provided some stability to the helix; however, phenylalanine−phenylalanine (F−F) and phenylalanine−pentafluorophenylalanine (F−f_5F) interactions resulted in the greatest enhancement in helicity, doubling the helical content over *i*, *i* + 5 control peptides at internal positions. Quantification of these interactions using AGADIR multistate helix-coil algorithm revealed that the F−F and F−f_5F interaction energies are equivalent at internal positions in the sequence ($\Delta G_{F-F} = \Delta G_{F-f5F} = -0.27$ kcal/mol), despite the differences in their expected geometries. As the strength of a face-to-face stacked phenyl−pentafluorophenyl interaction should surpass an edge-to-face or offset-stacked phenyl−phenyl interaction, we believe this result reflects the inability of the side chains in F−f_5F to attain a fully stacked geometry within the context of an α-helix. Positioning the interactions at the C-terminus led to much stronger interactions ($\Delta G_{F-F} = -0.8$ kcal/mol; $\Delta G_{F-f5F} = -0.55$ kcal/mol) likely because of favorable χ_1 rotameric preferences for aromatic residues at C-capping regions of α-helices, suggesting that aromatic side chain−side chain interactions are an effective α-helix C-capping method.

Introduction

The ability of specific side chain−side chain interactions to stabilize α-helical structure has been appreciated for several years. In particular, side chain−side chain interactions involving fundamental interactions such as hydrogen bonding, electrostatics, and hydrophobic packing have been shown to significantly enhance α-helicity in monomeric peptides.[1−8] Burley and Petsko were the first to suggest aromatic−aromatic interactions as an additional noncovalent interaction involved in protein structure stability.[9] Their statistical analysis of the aromatic side chains in the X-ray structures of 34 proteins revealed stabilizing interactions between −1 and −2 kcal/mol with dihedral angles often approaching 90°. In addition, the prevalence of aromatic interactions was high, occurring in 60% of all aromatic side chains in the protein data set. More recently, Serrano and coworkers determined the energy contribution of *i*, *i* + 4 Tyr−Tyr and Phe−Phe interactions at a solvent-exposed face of an α-helix in Barnase.[10] Using a double-mutant cycle, they determined that Tyr−Tyr and Phe−Phe interactions contribute an equivalent −1.3 kcal/mol to the stability of the protein, albeit in the presence of other side chain−side chain interactions with Tyr or Phe.

As of yet, the source of attraction between aromatics is not well understood. Much effort has gone into determining the dominant force controlling the interaction. Experimental and theoretical studies indicate that the strength of aromatic−aromatic interactions may be tuned through hydrophobic[11−13] and van der Waals forces,[14,15] as well as electrostatics.[16−18] The hydrophobic and van der Waals components of the interaction lead to stronger interactions between aromatic systems with more hydrophobic or π surface area in water, while the electrostatic component is proposed to give rise to a geometric preference to the interaction. Hunter and Sanders have rationalized the geometries of aromatic−aromatic interactions

* Address correspondence to this author. E-mail: mlwaters@email.unc.edu.

(1) Stapley, B. J.; Doig, A. J. *J. Mol. Biol.* **1997**, *272*, 465−473.
(2) Huyghues-Despointes, B. M. P.; Klinger, T. M.; Baldwin, R. L. *Biochemistry* **1995**, *34*, 13267−13271.
(3) Scholtz, M.; Qian, H.; Robbins, V. H.; Baldwin, R. L. *Biochemistry* **1993**, *32*, 9668−9676.
(4) Smith, J. S.; Scholtz, J. M. *Biochemistry* **1998**, *37*, 33−40.
(5) Viguera, A. R.; Serrano, L. *Biochemistry* **1995**, *34*, 8771−8779.
(6) Stapley, B. J.; Rohl, C. A.; Doig, A. J. *Protein Sci.* **1995**, *4*, 2383−2391.
(7) Padmanabhan, S.; Baldwin, R. L. *J. Mol. Biol.* **1994**, *241*, 706−713.
(8) Padmanabhan, S.; Jimenez, M. A.; Laurents, D. V.; Rico, M. *Biochemistry* **1998**, *37*, 17318−17330.
(9) Burley, S. K.; Petsko, G. A. *Science* **1985**, *229*, 23−28.
(10) Serrano, L.; Bycroft, M.; Fersht, A. R. *J. Mol. Biol.* **1991**, *218*, 465−475.
(11) (a) Newcomb, L. F.; Gellman, S. H. *J. Am. Chem. Soc.* **1994**, *116*, 4993−4994. (b) Gellman, S. H.; Haque, T. S.; Newcomb, L. F. *Biophys. J.* **1996**, *71*, 3523−3525.
(12) Guckian, K. M.; Schweitzer, B. A.; Ren, R. X. F.; Shiels, C. J.; Tahmassebi, D. C.; Kool, E. T. *J. Am. Chem. Soc.* **2001**, *122*, 2213−2222.
(13) Cubberley, M. S.; Iverson, B. L. *J. Am. Chem. Soc.* **2001**, *123*, 7560−7563.
(14) (a) Kim, E.; Paliwal, S.; Wilcox, C. S. *J. Am. Chem. Soc.* **1998**, *120*, 11192−11193. (b) Paliwal, S.; Geib, S.; Wilcox, C. S. *J. Am. Chem. Soc.* **1994**, *116*, 4497−4498.
(15) (a) Jorgensen, W. L.; Severance, D. L. *J. Am. Chem. Soc.* **1990**, *112*, 4768−4774. (b) Tsuzuki, S.; Honda, K.; Uchimaru, T.; Mikami, M.; Tanabe, K. *J. Am. Chem. Soc.* **2002**, *124*, 104−112.
(16) (a) Hunter, C. A.; Sanders, J. K. M. *J. Am. Chem. Soc.* **1990**, *112*, 5525−5534. (b) Hunter, C. A.; Lawson, K. R.; Perkins, J.; Urch, C. J. *J. Chem. Soc., Perkin Trans.* **2001**, 651−669. (c) Carver, F. J.; Hunter, C. A. *Chem. Commun.* **1998**, *7*, 775−776.
(17) Rashkin, M. J.; Waters, M. L. *J. Am. Chem. Soc.* **2002**, *124*, 1860−1861.
(18) Cozzi, F.; Siegel, J. S. *Pure Appl. Chem.* **1995**, *67*, 683−689.

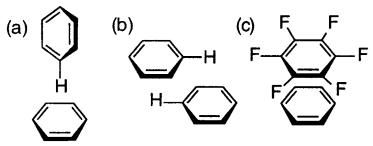

Figure 1. Geometries of aromatic interactions (a) edge-face; (b) offset-stacked; (c) face-to-face stacked.

through a model that relies upon the quadrupole moment of benzene which arises from the positively charged σ-framework between two regions of π-electron density on the faces of the ring.[16] As a result of the quadrupole, a face-to-face stacking arrangement for a benzene−benzene interaction is repulsive, whereas edge-to-face or offset-stacked interactions are favored (Figure 1). The strong face-to-face stacking interaction of benzene and hexafluorobenzene, which has been exploited to control recognition in supramolecular systems,[19] may be explained by a reversal of the quadrupole moment of hexafluorobenzene because of the electron-withdrawing fluorine substituents, allowing a net electrostatic attraction between the π-faces to occur. Gas phase theoretical estimates for the benzene−hexafluorobenzene interaction predict a stabilization energy of 3.7 kcal/mol at 3.6 Å separation.[20]

Although aromatic−aromatic interactions are now recognized as a significant contributor to native protein structure,[21] there has not been a quantitative experimental evaluation of these side chain−side chain interactions in model α-helical peptides, free from potential interference from tertiary contacts. Several groups have used Ala-Lys or Ala-Gln host sequences to identify helix stabilizing side chain−side chain interactions.[22] Most relevant to this study, Phe−His^+ and Trp−His^+ aromatic−amino interactions[23] and aromatic interactions between pairs of unnatural ϵ-(3,5-dinitrobenzoyl)Lys residues[24] have been shown to significantly promote α-helical structure as determined by circular dichroism (CD). However, the quantification of side chain interactions in monomeric peptide helices is complicated because of the multistate nature of the helix-coil transition. Accurate quantification of side chain interactions requires the use of helix-coil transition models, such as AGADIR[25] and modified Lifson−Roig[26] theories, equipped to account for energy contributions from side chain−side chain interactions. Typical side chain-side chain interaction energies are in the range of −0.2 to −1 kcal/mol, where applications of helix-coil theories are reported.[1−6,8,27] In the present work, the ability of natural and unnatural *i*, *i* + 4 aromatic interactions to stabilize an Ala-Lys based α-helix were measured by CD, and the interactions were quantified using the most recent version of the program AGADIR.

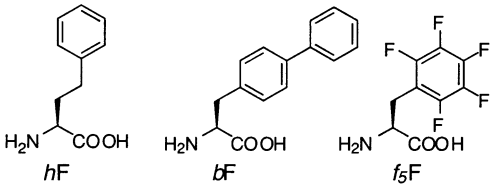

Figure 2. Structures of unnatural L aromatic amino acids. Abbreviations: *h*F = homophenylalanine, *b*F = biphenylalanine, f_5F = pentafluorophenylalanine.

We have investigated four Phe−X side chain−side chain interactions, where Phe is paired with itself (F−F), homophenylalanine (F−*h*F), biphenylalanine (F−*b*F), or pentafluorophenylalanine (F−f_5F) (Figure 2) in an *i*, *i* + 4 arrangement, initially at internal positions of an α-helix. The use of unnatural side chains has allowed us to probe the influence of side chain length and flexibility (F−*h*F), π-surface area (F−*b*F), and electronics (F−f_5F) on the strength of the aromatic side chain−side chain interaction. The present investigation not only provides further evidence for the involvement of aromatic interactions in protein structure stability, but also, with the use of unnatural aromatic side chains, investigates some of the structural factors that influence the strength of aromatic interactions within the context of an α-helix. In addition, the position dependence of aromatic interactions is investigated by moving the F−F and F−f_5F interactions to the C-terminus. Rotamer preferences for aromatic side chains in α-helices indicate that aromatic interactions will be limited at internal positions of the helix.[28] A study on the position dependence of a Phe−His^+ interaction in α-helical peptides has suggested that the interaction is strongest at the C-terminus where the optimal rotamer orientations for the interacting side chains is most feasible.[25e] Our results provide further evidence for this effect.

Experimental Procedures

Peptide Synthesis and Purification. Peptides were synthesized by automated solid-phase peptide synthesis on an Applied Biosystems Pioneer Peptide Synthesizer using Fmoc protected amino acids on a PEG-PAL-PS resin. Unnatural amino acids (homophenylalanine, biphenylalanine, and pentafluorophenylalanine) were purchased from Synthetech, Inc. The amino acid residues were activated for coupling with HBTU (O-benzotriazole-N,N,N′,N′,-tetramethyluronium hexafluorophosphate) and HOBT (N-hydroxybenzotriazole) in the presence of DIPEA (diisopropylethylamine). Deprotections were carried out in 2% DBU (1,8-diazabicyclo[5.4.0]undec-7-ene), 2% piperidine in DMF (*N*,*N*-dimethyl formamide) for approximately 10 min. Standard coupling cycles were used for the first 9−12 couplings (45 min) and extended coupling cycles (1 h, 15 min) were used to complete the sequence. The N-terminus was acetylated with 5% acetic anhydride, 6% 2,6-lutidine in DMF for 30 min. Cleavage of the peptide from the resin was performed in 95:2.5:2.5 Trifluoroacetic acid (TFA):Triisopropylsilane (TIPS):water for 3−4 h. TFA was evaporated and cleavage products were dissolved in ether. The water-soluble peptides were

(19) (a) Ponzini, F.; Zagha, R.; Hardcastle, K.; Siegel, J. S. *Angew. Chem., Int. Ed.* **2000**, *39*, 2323−2325. (b) Coates, G. W.; Dunn, A. R.; Henling, L. M.; Ziller, J. W.; Lobkovsky, E. B.; Grubbs, R. H. *J. Am. Chem. Soc.* **1998**, *120*, 3641−3649. (c) Coates, G. W.; Dunn, A. R.; Henling, L. M.; Dougherty, D. A.; Grubbs, R. H. *Angew. Chem., Int. Ed. Engl.* **1997**, *36*, 248−251.
(20) West, A. P., Jr.; Mecozzi, S.; Dougherty, D. A. *J. Phys. Org. Chem.* **1997**, *10*, 347−350.
(21) McGaughey, G. B.; Gagne, M.; Rappe, A. K. *J. Biol. Chem.* **1998**, *273*, 15458−15463.
(22) Chakrabartty, A.; Baldwin, R. L. *Adv. Protein Chem.* **1995**, *16*, 141−176.
(23) (a) Armstrong, K. M.; Fairman, R.; Baldwin, R. L. *J. Mol. Biol.* **1993**, *230*, 284−291. (b) Fernandez-Recio, J.; Vasquez, A.; Civera, C.; Sevilla, P.; Sancho, J. *J. Mol. Biol.* **1997**, *267*, 184−187.
(24) Albert, J. S.; Hamilton, A. D. *Biochemistry* **1995**, *34*, 984−990.
(25) (a) Munoz, V.; Serrano, L. *Nat. Struct. Biol.* **1994**, *1*, 399−409. (b) Munoz, V.; Serrano, L. *J. Mol. Biol.* **1994**, *245*, 275−296. (c) Munoz, V.; Serrano, L. *J. Mol. Biol.* **1994**, *245*, 297−308. (d) Munoz, V.; Serrano, L. *Biopolymers* **1997**, *41*, 297−308. (e) Lacroix, E.; Viguera, A. R.; Serrano, L. *J. Mol. Biol.* **1998**, *284*, 173−191.
(26) (a) Doig, A. J.; Chakrabartty, A.; Klinger, T. M.; Baldwin, R. L. *Biochemistry* **1994**, *33*, 3396−3403. (b) Kallenbach, N. R.; Lyu, P. C.; Zhou, H. X. In *Circular Dichroism and the Helix-Coil Transition in Peptides and Polypeptides*; Fasman, G. D., Ed.; Plenum Press: New York, 1996; pp 201−259.
(27) (a) Shi, Z.; Olson, C. A.; Kallenbach, N. R. *J. Am. Chem. Soc.* **2002**, *124*, 3284−3291. (b) Olson, C. A.; Shi, A.; Kallenbach, N. R. *J. Am. Chem. Soc.* **2001**, *123*, 6451−6452.
(28) (a) Stapley, B. J.; Doig, A. J. *J. Mol. Biol.* **1997**, *272*, 456−464. (b) Prieto, J.; Serrano, L. *J. Mol. Biol.* **1997**, *274*, 276−288.

extracted with water and lyophilized. Peptides were purified by reversed phase HPLC, using a Vydac C-18 column and a gradient of 0 to 60% B in 50 min, where solvent A was 95:5 water:acetonitrile, 0.1% TFA and solvent B was 95:5 acetonitrile:water, 0.1% TFA. The identity of each peptide was confirmed by MALDI mass spectrometry.

Determination of $\epsilon_{bF,275}$. The extinction coefficient of *b*F at 275 nm was determined by UV/Vis spectroscopy from tripeptide K-*b*F−K−NH_2 in 10 mM sodium phosphate, 100 mM sodium chloride, pH 7.5 buffer. ($\epsilon_{275} = 11\,200\ M^{-1}cm^{-1}$).

CD Measurements. Stock solutions of the purified peptides were prepared by dissolving in 10 mM sodium phosphate, 100 mM sodium chloride, pH 7.5 buffer. The concentration of each peptide was then determined in 5 M guanidinium hydrochloride using the absorbance of the tyrosine residue at 275 nm ($\epsilon = 1450\ M^{-1}cm^{-1}$).[29] Concentrations of peptides containing biphenylalanine were determined using both tyrosine and biphenylalanine side chain absorbances at 275 nm ($\epsilon_{bF,275} = 11200\ M^{-1}cm^{-1}$). Pentafluorophenylalanine does not absorb at 275 nm and thus does not interfere with concentration measurements. Peptides were diluted with buffer to give a known final concentration in the range of 70−120 μM. Three samples were prepared for each peptide to enable an error determination for fraction helicities caused by errors in the concentration measurements. CD spectra were acquired on an Aviv 60DS spectropolarimeter and scans were taken from 250 to 190 nm at 0−1 °C. Helical contents were determined for three samples of each peptide from the mean residue ellipticity at 222 nm, $[\theta]_{222,obs}$, and were calculated according to fraction helix (f_H) = $([\theta]_{222,obs} - [\theta]_{222,0})/([\theta]_{222,100} - [\theta]_{222,0})$. Values used for 0% and 100% helicity, $[\theta]_{222,0}$ and $[\theta]_{222,100}$, were +640 deg cm^2/dmol and −40000(1−2.5/*n*), respectively, where *n* is the number of residue units.[6,8]

Concentration Dependence Studies. Concentration dependence studies were carried out for the peptides to determine their aggregation state. Solutions of the peptide in buffer were prepared at several concentrations between 5 and 600 μM. $[\theta]_{222}$ was determined for each solution by CD, and no change with concentration was observed, indicating that the peptides are monomeric.

Determination of Interaction Energies. Analysis of the free-energy contribution of the side chain−side chain interactions was determined using the most recent version of the program AGADIR.[25] The AGADIR helix-coil transition model uses two basic parameters to describe helix nucleation and propagation. Helix propensities are expressed by $h_n = \exp-(\Delta G_{intri}/RT)$ where ΔG_{intri} is the intrinsic helix forming free energy for a specified residue. The mean residue enthalpic contribution for α-helix formation is $h_e = \exp-(\Delta G_{Hbond}/RT)$, where ΔG_{Hbond} is an energy term for the formation of an intramolecular hydrogen bond. Helix-coil cooperativity is modeled by assuming each residue either nucleating or elongating the helix is associated with a parameter h_n, and only those elongating the helix (all residues but those forming the first turn) hold an additional parameter h_e. AGADIR also accounts for any stabilizing side chain interactions that may be present within the host sequence. To determine the free energy of a specified side chain−side chain interaction, the helicity of the sequence is predicted by AGADIR, initially setting the desired side chain−side chain interaction energy to zero. If any additional helix stability is experimentally observed in the sequence, that stability is attributed to the side chain interaction energy. The side chain−side chain interaction energy is then varied until the predicted AGADIR helicity for the *i*, *i* + 4 peptide matches the experimental values. As a control, the helicities of the *i*,*i* + 5 peptides were also determined by AGADIR and shown to correspond with the experimentally determined helicities.

Results and Discussion

Peptide Design. The peptide sequences used for investigating aromatic interactions are shown in Figure 3. Each peptide has the general host sequence $(AAKAA)_n$,[29] where the high helix propensity of alanine supplies the peptides with a tendency to form a helix, and the *i*, *i* + 5 spaced Lys residues allow for water solubility and prevent peptide aggregation. The *i*, *i* + 4 spaced F−F, F−*h*F, and F−*b*F interactions were investigated in the host sequence **F7X11**. The *i*, *i* + 4 F−f_5F interaction was studied in a longer host sequence **F12X16** because of the helix-breaking character of the f_5F residue. The corresponding *i*, *i* + 5 control peptides were also synthesized for each interaction studied in which the aromatic side chains are located on opposite sides of the helix, preventing an interaction. The C-terminal *i*, *i* + 4 F−F and F−f_5F interactions were investigated in host sequence **cF13X17**. Peptide **A7X11** was used to determine the helix propensities for the unnatural amino acids. All peptide sequences displayed characteristic α-helical CD spectra, with minima near 208 and 222 nm. CD concentration dependence studies between 5 and 600 μM indicate that these peptides are monomeric.

(a) **F7X11** Ac-YGGKAA**F**AKA**X**AAKAAAAK-NH_2 *i*, *i* + 4
F6X11 Ac-YGGKA**F**AAKA**X**AAKAAAAK-NH_2 *i*, *i* + 5
X = F, *h*F, *b*F

(b) **F12X16** Ac-YGGKAAAAKAA**F**AKA**X**AAKAAAAK-NH_2 *i*, *i* + 4
F11X16 Ac-YGGKAAAAKA**F**AAKA**X**AAKAAAAK-NH_2 *i*, *i* + 5
X = f_5F

(c) **cF13X17** Ac-YGGAKAAAAKAA**F**AKA**X**A-NH_2 *i*, *i* + 4
X = F, f_5F

(d) **A7X11** Ac-YGGKAA**A**AKA**X**AAKAAAAK-NH_2
X = A, F, *b*F, *h*F

Figure 3. Peptide sequences used to study aromatic side chain interactions. (a) 19-residue sequences with Phe−X interactions at an internal position. (b) The 24-residue sequences for the investigation of the F−f_5F interaction at an internal position. (c) The 18-residue sequence with a C-terminal *i*, *i* + 4 aromatic interaction. (d) Sequence used to determine helix propensities. Abbreviations: A = alanine, F = phenylalanine, G = glycine, Y = tyrosine, K = lysine, *h*F = homophenylalanine, *b*F = biphenylalanine, f_5F = pentafluorophenylalanine, Ac = acetyl.

Determination of Intrinsic Helix Propensities for the Unnatural Amino Acids. To quantify the side chain−side chain interactions by AGADIR, the helix propensities of the unnatural amino acids were determined. This allowed for the separation of differences in helix stability arising from intrinsic structural properties of the individual side chains from those resulting from side chain−side chain interactions. With the exception of f_5F, the helix propensities of the unnatural amino acids were determined from the change in helicity resulting from an Ala to X substitution in peptide **A7X11** (Figure 3d), where X is the unnatural residue. This change was fit by AGADIR theory to give a helix propensity (ΔG_{intri}) reported in kcal/mol (Table 1). Because the helicity of **A7*f*$_5$F11** was below 15%, the helix propensity for f_5F was determined directly from the *i*, *i* + 5 control peptide, **F11*f*$_5$F16**. The helix propensities were converted to their corresponding Zimm−Bragg *s*-values for comparison. The *s*-values in Table 1 correlate well with previously determined helix propensities for aromatic residues.[29] The order of helix propensities for the aromatic residues is f_5F < *b*F < F < *h*F, with f_5F being the most helix-breaking residue. This ordering is reasonable as bulky, branched side chains typically have lower helix propensities.[22] These helix propensities were shown to accurately predict the helicities of the *i*, *i* + 5 control peptides by AGADIR.

(29) (a) Chakrabarty, A.; Kortemme, T.; Baldwin, R. L. *Protein Sci*. **1994**, *3*, 843−852. (b) Padmanabhan, S.; York, E. J.; Stewart, J. M.; Baldwin, R. L. *J. Mol. Biol*. **1996**, *257*, 726−734.

Table 1. Helix Propensities for Unnatural Aromatic Amino Acids[a]

X	$[\theta]_{222}$[b] (deg·cm²/dmol)	f_H[c]	AGADIR ΔG_{intri} (kcal/mol)	Zimm–Bragg *s*-value[d]
A	−18900	.55		
*h*F	−15900	.47	0.96	.87
*b*F	−10400	.31	1.41	.38
f_5F	−11100	.32	1.49	.33
F	−11000	.33	1.38	.40

[a] The helix propensities were determined from **A7 X11** with the exception of f_5F, which was determined from **F11X16**. [b] In 10 mM sodium phosphate, 100 mM sodium chloride, pH 7.5 buffer at 0−1 °C. [c] Helical contents were calculated according to $f_H = ([\theta]_{222} - [\theta]_{222,0})/([\theta]_{222,100} - [\theta]_{222,0})$ where $[\theta]_{222,0}$ and $[\theta]_{222,100}$ represent $[\theta]_{222}$ for 0 and 100% helical contents, respectively. $[\theta]_{222,0} = +640$ deg·cm²/dmol and $[\theta]_{222,100} = -40000(1-2.5/n)$ deg·cm²/dmol where n is the number of residue units. The error in helical contents is ±3% (see Experimental Section for error determination). [d] The relationship between AGADIR ΔG_{intri} and Zimm−Bragg *s*-values is $s = \exp-[(\Delta G_{intri} + \Delta G_{Hbond})/RT]$ where ΔG_{Hbond} is −0.882 kcal/mol in AGADIR for this series of peptides.[25d]

Table 2. Circular Dichroism Data, Fractional Helicities, and ΔG's for *i*, *i* + 4 Interactions

peptide	spacing	$[\theta]_{222}$[a] deg·cm²/dmol	f_H	ΔG[c] kcal/mol
F7F11	*i*, *i* + 4	−6800	.21	−0.27
F6F11	*i*, *i* + 5	−3400	.11	
F7*h*F11	*i*, *i* + 4	−13500	.40	−0.18
F6*h*F11	*i*, *i* + 5	−9700	.29	
F7*b*F11[b]	*i*, *i* + 4	−6700	.21	−0.10
F6*b*F11[b]	*i*, *i* + 5	−5700	.18	
F12f_5F16	*i*, *i* + 4	−20500	.58	−0.27
F11f_5F16	*i*, *i* + 5	−11100	.32	
cF13F17	*i*, *i* + 4	−9400	.29	−0.80
cF13f_5F17	*i*, *i* + 4	−5800	.19	−0.55

[a] The conditions are the same as in Table 1. [b] The concentration of peptides containing *b*F were calculated by accounting for the *b*F absorbance at 275 nm ($\epsilon_{275,bF} = 11\,200\ M^{-1}\ cm^{-1}$). [c] In AGADIR, there is a favorable *i*, *i* + 3 Phe−Lys interaction when Phe is N-terminal.[25a]

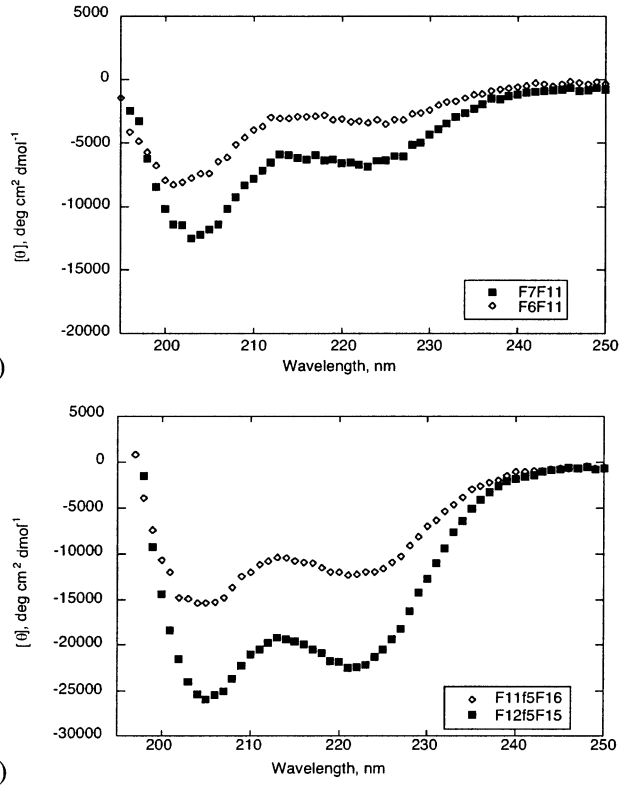

Figure 4. Overlaid circular dichroism spectra of peptides. (a) **F7F11** (squares) and **F6F11** (diamonds) and (b) **F12f_5F16** (squares) and **F11f_5F16** (diamonds) in 10 mM phosphate buffer, 100 mM sodium chloride, pH 7.5 at 0−1 °C. Peptide concentrations were 70−120 μM as determined by Tyr absorbance at 275 nm.

Aromatic Interactions at Internal Positions in the α-Helix. All of the *i*, *i* + 4 peptides incorporating aromatic interactions at internal positions showed higher helical contents than their respective *i*, *i* + 5 controls by CD (Table 2).[30] In particular, the *i*, *i* + 4 F−F and F−f_5F peptides were twice as helical as their corresponding controls, suggesting that aromatic side chain−side chain interactions have a significant influence on the stability of α-helix structure (Figure 4).

The side chain−side chain interaction energies were determined by fitting the experimental helicities with the AGADIR helix-coil transition algorithm (Table 2). The results demonstrate that the *i*, *i* + 4 F−F and F−f_5F interactions are equally stabilizing, which is surprising since the preferred geometries of the two aromatic pairs differ greatly. Two phenyl rings form favorable interactions in both the offset-stacked and edge-to-face geometries, whereas a phenyl−pentafluorophenyl interaction prefers the fully stacked conformation to maximize the nearly equal and opposite quadrupole−quadrupole interaction (Figure 1).[16,20] Molecular modeling has suggested that the *i*, *i* + 4 F−F interaction can access both offset-stacked and edge-to-face geometries but not the face-to-face geometry (data not shown). We expect that the F−f_5F interaction shows no enhanced stabilization over the F−F interaction because of an inability to access the ideal fully stacked geometry in the α-helix. On the basis of an electrostatic model, Phe and f_5F are expected to interact in a repulsive manner in the edge-face geometry, and there is some experimental evidence for this in model systems.[31] However, pentafluorophenyl amides have been observed to interact with phenylamides in the offset-stacked geometry in the solid state, suggesting that this is likely the orientation of the rings in this system that gives rise to helix stabilization.[31]

Although both **F7*h*F11** and **F7*b*F11** are also more helical than their *i*, *i* + 5 controls, the F−*h*F and F−*b*F interactions provide less stability to the helix than the F−F and F−f_5F interactions. The F−*h*F interaction may experience a greater entropic cost to confine the residues in the optimal geometry for an interaction. The larger surface area of *b*F may actually disfavor an aromatic side chain−side chain interaction by favoring a rotamer that allows the biphenyl to pack against the helix backbone.

Aromatic Interactions at the C-terminus of the α-Helix. Previous work on a Phe−His^+ interaction in α-helical peptides has indicated a position dependence for the strength of the interaction. It has been suggested that the optimal geometry of an *i*, *i* + 4 Phe−His^+ interaction within an α-helix requires that the Phe side chain adopts the trans rotamer ($\chi_1 = 180°$) and the *i* + 4 His^+ side chain adopts the gauche$^+$ rotamer ($\chi_1 = -60°$).[25e] This combination orients the side chains toward one another in an edge-to-face conformation, where the edge NH or CH of His^+ ring is directed to the face of the phenyl ring. This geometry has been observed in the crystal structure

(30) Since the N-terminal YGG residues likely do not contribute to the helix, F7 is at the fourth position in the helix. However, hydrophobic residues in this position have been shown to behave equivalently to an internal position. See (a) Petukhov, M.; Munoz, V.; Yumoto, N.; Yoshikawa, S.; Serrano, L. *J. Mol. Biol.* **1998**, *278*, 279−289. (b) Penel, S.; Hughes, E.; Doig, A. J. *J. Mol. Biol.* **1999**, *287*, 127−143.

(31) Adams, H.; Blanco, J. L. J.; Chessari, G.; Hunter, C. A.; Low, C. M. R.; Sanderson, J. M.; Vinter, J. G. *Chem. Eur. J.* **2001**, *7*, 3494−3503.

Table 3. Experimental Energies for Side Chain Interactions in α-Helices

entry	interaction (N to C)	ΔG kcal/mol	algorithm	reference
1	Leu−Tyr	−1.0	Lifson−Roig	8
2	Phe−Met	−0.65	AGADIR	5
3	Phe−Met	−0.75	Lifson−Roig	6
4	Trp−His^+	−0.8	AGADIR	23b
5	Gln−Asn	−0.4 to −0.7	Lifson−Roig	1
6	Lys^+−Asp	−0.58	Lifson−Roig	4
7	His^+−Glu	−0.65	Lifson−Roig	4
8	[a]Phe−His^+	−0.4	AGADIR	25e
9	Trp−Arg^+	−0.4	Zimm Bragg	27a
10	Glu^-−Phe	−0.55	Zimm Bragg	27b

[a] Interaction energy is correct when His^+ is at position C1 or Ccap.

of the C-terminal Phe−His^+ interaction in Ribonuclease A.[23a] However, the preferred rotamer orientation for aromatic residues is trans in α-helical regions of proteins[28a] and approaches gauche$^+$ at C-terminal and C-capping regions of α-helices.[28b] Lacroix et al. have found that the Phe−His^+ interaction reported by Baldwin and co-workers[23a] is three times stronger when His^+ is located at position C1 or Ccap, where it can attain its optimal rotamer orientation for interaction with Phe.[25e] Recently, there has been some debate over whether this effect is truly due to rotamer preferences, or if it is simply the result of the greater accessibility of the His^+ residue to solvent at the C-terminus.[32] A more solvent-exposed His^+ residue is more likely to be protonated, thus strengthening the Phe−His^+ aromatic−amino interaction. We expected that if the result reported by Lacroix et al. was due to rotamer preferences and not solvation effects, we would see a similar increase in strength for a C-terminal F−F interaction. Thus, we investigated the helix-stabilizing properties of *i*, *i* + 4 F−F and F−f_5F interactions at the C-terminus (Figure 3c).

Positioning the F−F interaction at the C-terminus in **cF13F17** does indeed raise the interaction energy by a factor of 3, indicating that preferred rotamer populations significantly limit the energetic contribution of aromatic interactions at internal positions of α-helices (Table 2).[33] This result also strongly suggests that the *i*, *i* + 4 F−F interaction, like the Phe−His^+ interaction in Ribonuclease A, interacts via an edge-to-face geometry. In contrast, the F−f_5F interaction increased by a factor of 2 at the C-terminus in peptide **cF13f_5F17**. This may be the result of different rotamer population distributions for the f_5F side chain. It is also likely that the F−f_5F interaction requires a different rotamer geometry than the F−F interaction.[31] In any case, the fact that any stabilization results from the F−f_5F interaction is surprising since it appears that a fully stacked interaction cannot be accessed within the context of an α-helix. It is possible that the F−f_5F interaction provides stability simply because of an increased hydrophobic interaction, as a pentafluorophenyl ring is more hydrophobic than a phenyl ring.[34]

Comparison to Previous Studies. Our results demonstrate that the naturally occurring *i*, *i* + 4 F−F interaction is the most effective aromatic side chain interaction for promoting α-helical structure in this study. We have shown that the F−F interaction can contribute as much as −0.8 kcal/mol to the stability of an α-helix. Experimental free energies for other side chain−side chain interactions are reported in Table 3 for comparison. The C-terminal F−F interaction is comparable in energy to Phe−Met[5,6] and Leu−Tyr[8] hydrophobic interactions and a Trp−His^+ amino−aromatic interaction.[23b] The F−F interaction appears to slightly surpass the energies of a Gln−Asn hydrogen bond[1] and the strongest salt bridges reported by Scholtz et al. (entries 6 and 7) in 0.01 M sodium chloride.[4] Interestingly, the F−F interaction is significantly more stabilizing than the C-terminal Phe−His^+ interaction as well as the cation-π (Trp−Arg^+) and anion-π (Glu^-−Phe) interactions recently reported by Kallenbach et al.[27] The fact that the C-terminal F−F interaction is more stabilizing at the solvent-exposed face of an α-helix than these related nonclassical noncovalent interactions is likely the result of the lower desolvation penalty for aromatic−aromatic interactions. Although there is expected to be a larger electrostatic component for anion-π and cation-π interactions, there is also a greater tendency for the charged side chains to be solvated by water.

Conclusions

We have presented the first quantitative experimental investigation of the fundamental role of aromatic interactions in monomeric α-helical structure. Our results have shown that a F−F interaction can stabilize an α-helix, but the strength is largely influenced by the rotamer populations of the interacting side chains, resulting in a much stronger interaction at the C-terminus than at the center of an α-helix. These results, along with those obtained from earlier studies on the Phe−His^+ interaction, indicate that aromatic interactions may present a general α-helix C-capping method involving side chain−side chain interactions, where the C-terminal aromatic side chain has the proper rotameric freedom to engage in a stabilizing interaction with another *i*-4 aromatic side chain.[35] Even at an internal position, however, we have found that an aromatic interaction can have a dramatic effect on the extent of folding, increasing overall helicity by a factor of 2 relative to *i*, *i* + 5 spaced controls in peptides **F7F11** and **F12f_5F16**. We expect that these results will allow a deeper understanding of aromatic interactions as an additional force that influences helix formation in water and will be applicable to the field of de novo protein design.

Acknowledgment. We thank Professor Luis Serrano for helpful discussions and assistance with the AGADIR calculations. We gratefully acknowledge the University of North Carolina College of Arts and Sciences for start-up funds. This work was supported by the Petroleum Research Fund (Grant number 35438-G4).

JA026668Q

(32) Bhattacharyya, R.; Samanta, U.; Chakrabarti, P. *Protein Eng.* **2002**, *15*, 91−100.

(33) The observed position dependence of helix propensities for hydrophobic residues suggest that the differences between the internal and C-terminal Phe are negligible. See Petukhov, M.; Uegaki, K.; Yumoto, N.; Serrano, L. *Protein Sci.* **2002**, *11*, 766−777.

(34) Hansch, C.; Leo, A.; Hockman, D. *Exploring QSAR: Hydrophobic, Electronic, and Steric Constraints*; ACS Professional Reference Series; American Chemical Society: Washington, DC, 1995.

(35) For a review on helix capping, see Aurora, R.; Rose, G. D. *Protein Sci.* **1998**, *7*, 21−38.